Fluid inclusions in "superquartzites" of the Bural-Sardyk deposit (*East Sayan*)

M.G. Volkova [a,*], A.I. Nepomnyashchikh [a,b], A.M. Fedorov [a,b], A.M. Makhlyanova [a], N.V. Bryanskii [a,b]

[a] *A.P. Vinogradov Institute of Geochemistry, Siberian Branch of the Russian Academy of Sciences, ul. Favorskogo 1a, Irkutsk, 664033, Russia*
[b] *Irkutsk State University, ul. Karla Marksa 1, Irkutsk, 664003, Russia*

Abstract

We present results of study of fluid inclusions in "superquartzites" of the Bural-Sardyk deposit (East Sayan). "Superquartzites" are regarded as a source of extrapure quartz raw material; therefore, the presence of fluid inclusions in them is an important characteristics of their quality. We have first applied not only microthermometry but also LA–ICP-MS to study fluid inclusions in the above rocks. Release of volatiles in quartzite grit was studied by thermal-desorption mass spectrometry. The research has shown the uneven distribution of fluid inclusions in the quartz grains. The inclusions are flattened isometric or rounded (often, of complex morphology), up to 12 μm across. The concentration of salts in the fluid corresponds to 5.5–5.7 wt.% NaCl equiv., Na is the main element in its salt system, and K and Mg are present in background concentrations. According to mass-spectrometric analysis, water is the main volatile component in the "superquartzite" (39 to 124 ppm). Next in abundance are carbon-containing substances (CO, CO_2, and hydrocarbons). On stepwise heating of the samples, H_2O releases in two temperature regions: at low temperatures (with the maximum release at 400 ºC) and at high temperatures (above 1000 ºC). The results of the chemical enrichment of "superquartzites" indicate low initial contents of structural impurities, which expands the boundaries for the application of this type of raw material in the production of high-tech quartz products.
© 2017, V.S. Sobolev IGM, Siberian Branch of the RAS. Published by Elsevier B.V. All rights reserved.

Keywords: fluid inclusions; "superquartzites"; microthermometry; salt system of fluid; high-purity quartz products

Introduction

Quartzites of the Bural-Sardyk deposit are of big practical interest as a source of high-purity raw quartz for some industrial fields (Fedorov et al., 2012; Makrygina and Fedorov, 2013; Vorob'ev et al., 2003). The presence of fluid inclusions (FI) is one of the most important quality characteristics of natural quartz as a raw material, along with the contents of impurity elements and mineral inclusions.

We have first performed microthermometric studies of FI in the rocks from this deposit, using inductively coupled plasma mass spectrometry with laser ablation (LA–ICP-MS). We also present results of thermal-desorption mass spectrometry study of volatiles in quartzite grit.

Geology

There are about ten quartzite shows in the East Sayan quartzite-bearing province. The best studied show is in the Bural-Sardyk deposit located in the southeast of East Sayan, within the watershed ridge between the Oka and Urik Rivers. The geologic structure and models of formation of the deposit are described in detail elsewhere (Anfilogov et al., 2015; Fedorov et al., 2012; Makrygina and Fedorov, 2013; Vorob'ev et al., 2003). The deposit area is a series of NE striking ridges and hills separated from each other by recent deposits (Arzhannikova et al., 2013), with the main Bural-Sardyk peak (2778 m). Quartzites compose intercalates few tens to few hundreds of meters in thickness among the carbonate deposits of the Riphean cover of the Archean–Lower Proterozoic Gargan terrane (Kuznetsov et al., 2010). The thickest quartzite members are observed on the northwestern periphery of the terrane. The productive bodies are monoquartzites; the degree of their recrystallization decreases from top to bottom of the section. They are localized as beds of gentle (7º–10º) W–NW

* Corresponding author.
E-mail address: volkova@igc.irk.ru (M.G. Volkova)

dip near the peak of the Bural-Sardyk Ridge. The upper section is composed of the maximally reworked "superquartzites" (Vorob'ev et al., 2003) and bleached fine-grained quartzites. The lower section consists of dark gray quartzites and a thin member of highly carbonaceous schungite-like bodies.

The "superquartzites" have a virtually monomineral quartz composition and an inequigranular allotriomorphic structure. Besides opaque fine-grained quartz aggregate, the rock contains coarse transparent quartz grains of subparallel orientation, with flexuous castellated edges and undulatory cloud-mosaic extinction. The rock is formed by coarse and medium quartz grains (5–50 vol.%) measuring 1.6×0.5 to 4×2 mm (seldom, to 9.4 mm) along the long axis. The fine grains (0.5×0.3 to 1.4×0.6 mm) are irregular-shaped, sometimes elongate, with rough castellated edges. The rock contains scarce sericite flakes. There are also thin carbonaceous veinlets in the interstices.

Quartzites of the Bural-Sardyk deposit can be divided into two groups according to the contents of major, trace, and rare-earth elements (Fedorov et al., 2012). The first group includes quartzites of the "productive unit": black and dark gray flint-like quartzites, fine-grained light quartzites, and "superquartzites", having low contents of major and trace elements. The second group is quartzites in contact with intrusive bodies. Their contents of major and trace elements are two orders of magnitude higher than those of the first-group quartzites (Fedorov et al., 2012). Granitoids of the Gargan pluton of the Sumsunur complex (785 Ma) are the most widespread intrusive bodies in this area. They were interpreted by Kuzmichev et al. (2004) and Kuzmichev and Larionov (2011) as suprasubductional.

Methods

Fluid inclusions were studied by *microcryothermometry* in double-side polished transparent plates. The search for FI and photography of the preparations were made in both transmitted and reflected light, using an Olympus BX 51 microscope equipped with PixeLink 1394 and QImagingMicroPublisher 5.0 RTV cameras. For all studies, the plates were soaked in analytical-grade acetone, peeled off the glass, and washed with ethyl alcohol. After the visual examination, plate fragments (3×3 to 4×4 mm in size) with the most appropriate FI were mechanically separated.

The microcryothermometric parameters were measured on a Linkam THMSG-600 freezing/thermal stage (Common-Use Center of Isotope-Geochemical Studies of the Institute of Geochemistry, Irkutsk) permitting determination of phase transition temperatures in the range from –196 to +600 ℃. The measurement accuracy was ±0.1 ℃ in the temperature range from –20 to +80 ℃ and ±1 ℃ beyond it. The freezing stage was equipped with the LinkSys 32-DV control software. Two-phase FI larger than 5 µm were studied. The temperatures of total homogenization into liquid were measured at the time of the gas bubble disappearance during the heating of the

preparation on the thermal stage. The salt concentrations were calculated using the FLINCOR program (Brown, 1989) and data from Bodnar and Vityk (1994).

The contents of volatiles in "superquartzite" were determined by *kinetic thermal-desorption mass spectrometry with a quantitative analysis of the flows of substances* released into a high vacuum when the sample with the particular degree of dispersion was heated step-by-step from room temperature to 1400 ℃. The samples were prepared as quartz grit with the grain size of 174–450 µm. The technique of sample preparation for thermal-desorption mass spectrometry includes the following processes: manual crushing of quartz to a 50 mm fraction; washing; crushing to a 25 mm fraction; classification to a 5–25 mm fraction; chemical etching with 10% HCl; drying; and abrasion in a quartz grinder. The procedure was performed by V.A. Kreisberg at the Chemical Department of Moscow State University. The prepared sample was placed into an ampoule made of annealed quartz glass and was evacuated for 24 h. All weakly bound, physically adsorbed impurities were removed in a high vacuum (10^{-7}–10^{-8} torr) before the mass-spectrometric annealing. On the subsequent heating with a 200 ℃ step, the kinetics of water release was continuously recorded; at the isothermal steps, the entire mass spectrum of the released gaseous products was recorded (Kreisberg et al., 2007).

The composition of the aqueous solution of FI was also examined by *LA–ICP-MS*. Data were obtained on setup including a NexION 300D quadrupole mass spectrometer and an NWR-213 laser ablation platform (Common-Use Center for Isotope-Geochemical Studies, Institute of Geochemistry, Irkutsk). Signals were measured for fifty elements. The method parameters are given in Table 1.

Using LA for sampling in combination with a quadrupole mass spectrometer makes it possible to examine small FI (≤5 µm), reveal mineral phases in the deep layers of the material, and analyze the sample aerosol rapidly changing in composition.

The contents of impurity elements in quartz concentrates were determined by ICP MS. The weighted sample was treated with HNO_3 at high pressure and temperature in an autoclave to transfer it into the solution. The samples with hardly soluble elements were treated with an $HF + HNO_3$ mixture. To prevent the loss of boron, mannitol was added to the acid mixture, which binds boron into a complex compound. For subsequent concentration of impurities, the main element was removed as silicon tetrafluoride. The salts were converted into a nitric form by the treatment of the dry residue with HNO_3. To reduce the mutual influence of the elements, the resulted concentrated solution was diluted before the recording of spectra (Sokol'nikova and Vasil'eva, 2012). The measurements were made on a NexION 300D (Perkin Elmer, Canada) mass spectrometer.

The Iota STD and Iota 4 (Unimin, USA) quartz concentrates, widely used in the world for the production of transparent quartz glass (Bur'an et al., 2007), were taken as reference samples for monitoring the results of ICP MS analysis. The samples were digested in an $HF + HNO_3$ mixture

Table 1. LA-ICP-MS parameters

Laser parameters	Values
Laser	Nd:YAG (NWR-213)
Wavelength	213 nm
Pulse energy	9.36 J/cm^2
Pulse repetition rate	5 Hz
Number of pulses	400
Ablation spot diameter	50 μm
Pulse length	4 ns
ICP MS parameters	Value
Carrier-gas flow rate	0.6 L/min He
Carrier-gas flow rate	0.8 L/min Ar
Other gases: Plasma/Cool and Auxiliary Gas	18 L/min and 2 L/min Ar, respectively
Plasma power	1400 W

at high pressure and temperature in an autoclave, and the main element was removed as silicon tetrafluoride from the produced solution for the concentration of impurities. The mass spectrometer was calibrated by mass using IQC-026 Combined Quality Control Standard (Ultra Scientific, USA) multielement solutions and ICP Multielement Standard Solution X (MerckKGaA, Germany). A rhodium solution was used as an internal standard for monitoring the measurement of the signal intensity. Sample weighing was made with a first- or second-order analytical balance. Calibration plots were constructed using Multielement Solution 1-4 (SPEX CertiPrep, USA) standards.

The intralaboratory accuracy was controlled by analyses of parallel weighted samples and by repeated analyses of selected
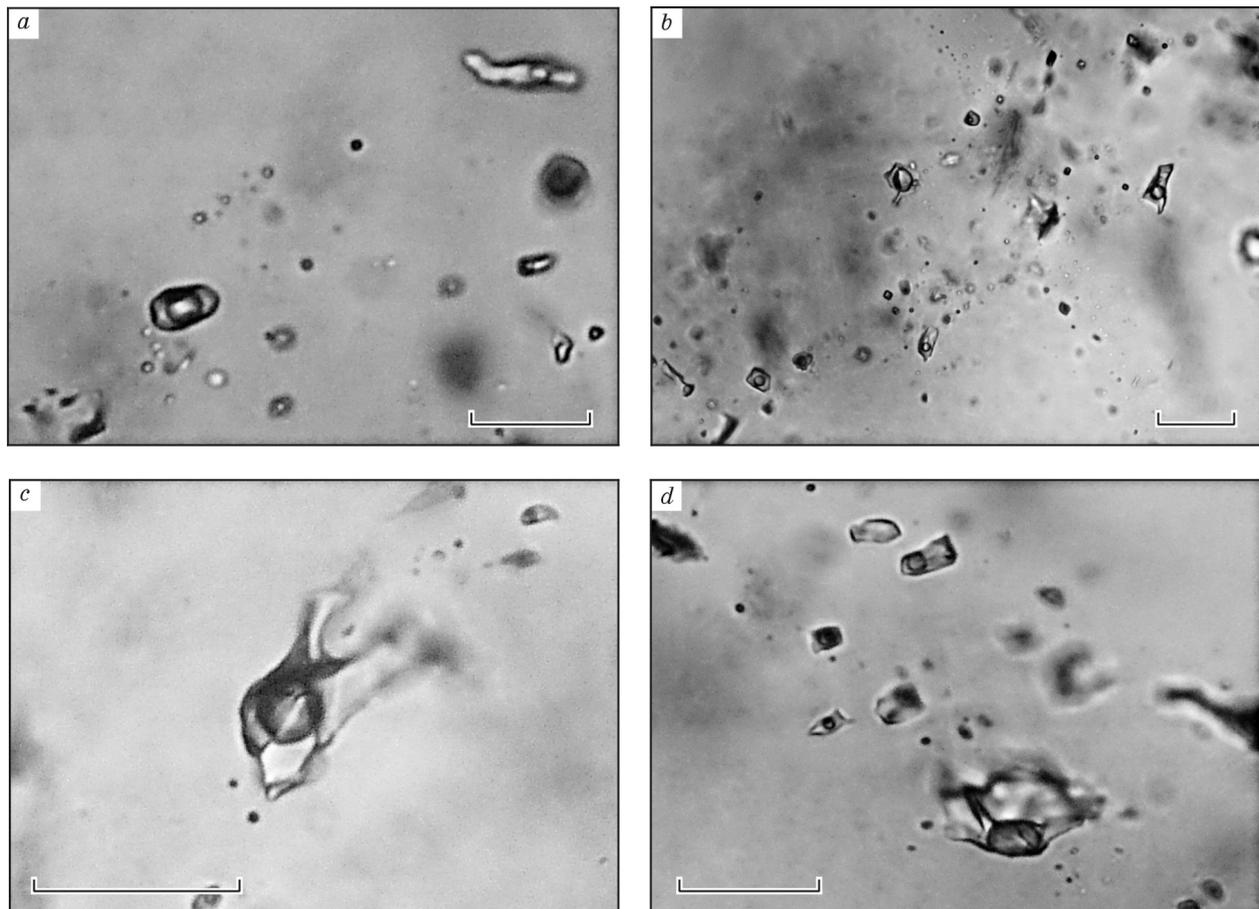

Fig. 1. Fluid inclusions in "superquartzites" from the Bural-Sardyk deposit (measured with a 10 μm scale bar). *a–d*, See description in the text.

Table 2. Results of microcriothermometric studies of fluid inclusions in "superquartzites" of the Bural-Sardyk deposit

Parameter	Value
Number of FI appropriate for measurements (n)	15
Inclusion size	up to 12 μm
Homogenization temperature of FI	235–247 ℃
Melting point of ice	–3.5 to –3.4 ℃
Salt concentration	5.5–5.7 wt.% NaCl equiv.

samples. The detection limits of elements were calculated following a standard procedure taking into account the results of the control experiments, the 3σ criterion, and the corresponding dilution of the solutions. To increase the accuracy of measurements and reduce the element concentrations, the control experiments were carried out with ultrapure reagents: acids purified by sub-boiling distillation and deionized water.

Results and discussion

We have established that FI are unevenly distributed within quartz grains. The cores of coarse and medium grains are poorer in FI than the edge zones and healed cracks. Fluid inclusions in fine quartz grains are smaller than 3 μm and are inappropriate for study. The inclusions form narrow chains passing into compact ribbon-like clusters 10 to 25 μm in size and then intersecting (Fig. 1b) or stretching parallel to each other or forming separate groups. They are flattened isometric rounded (Fig. 1a) or, most often, of complex morphology (Fig. 1b–d), ≤12 μm across (Fig. 1). The small size of FI makes their visual examination difficult and narrows the range of methods suitable for their analysis. At room temperature, a gas bubble occupies 25–50 vol.% of the inclusion vacuole (Fig. 1).

On rapid cooling to –100 ℃, the liquid in FI freezes. This process is poorly visible because of the small size of the inclusions; therefore, we failed to determine the exact eutectic temperature of their solutions. The melting point of ice was measured in 15 FI with a discernible liquid phase: It varies from –3.5 to –3.4 ℃ (Table 2). On heating, reduction in gas bubble volume in most of FI began at >150 ℃. The inclusions were totally homogenized into liquid within 235–247 ℃ (Table 2).

Calculations by the FLINCOR program (Brown, 1989) and by the technique from Bodnar and Vityk (1994) yielded a salt concentration of 5.5–5.7 wt.% NaCl equiv. in the fluids (Table 2).

Study by kinetic thermal-desorption mass spectrometry and a quantitative analysis of the substance flows (Table 3) showed that water is the main volatile (39–124 ppm) in the "superquartzite". Second in abundance are carbon-containing compounds (CO, CO_2, and hydrocarbons). The thermal-desorption curves (Fig. 2) demonstrate water release in two temperature regions. At low temperatures (with the maximum release at 400 ℃) it is due to decrepitation of vacuoles larger than 15 μm and surficial dehydration. At high temperatures, water release is related to diffusion of molecular-dispersed water in the quartz structure. After calcination at 1450 ℃, the "superquartzite" (sample 116/1) lacks high-temperature species of water and many other impurities but has a significant content of low-temperature water species (Fig. 2). This is due to the increase in the specific surface of the rock grains during cristobalitization and, correspondingly, due to adsorption of low-temperature water.

We performed an LA–ICP-MS analysis of the optically pure zones (free from fluid and mineral inclusions) of the "superquartzite" (Fig. 3, crater 1) and the zones with FI clusters (Fig. 3, crater 2). We had to examine these zones instead of individual FI because of the small size of the latter (Fig. 1). Though this local method permits study of objects up to 5 μm in size, the amount of substance in fine individual FI is insufficient for recording a stable analytical signal. Analysis of such objects was performed earlier, and adjustment of optimal parameters made it possible to achieve the effective ablation of the material (Makhlyanova et al., 2015).

Table 3. Contents of major volatiles in "superquartzite" (data of mass spectrometry analysis), ppm

Sample	H_2O			CO_2	CO	C_xH_x	ΣC	H_2	HCl	H_2S	SO_2
	<600 ℃	>600 ℃	Total								
	"Superquartzite" without thermal crushing										
78/1	58.2	65.7	123.9	2.4	9.4	3.7	7.9	0.21	1.87	0.78	0.15
	"Superquartzite" after thermal crushing*										
80/1	11.1	27.8	38.9	1.3	3.6	3.0	4.5	0.10	0.02	0.16	0.01
	"Superquartzite" after calcination at 1450 ℃**										
116/1	42.0	3.9	45.9	0.4	4.4	4.8	6.2	0.05	0.02	0.01	0.00
	Quartz concentrate Iota-STD (Unimin, USA)										
	18.6	17.2	35.8	1.3	4.5	3.9	5.7	0.51	0.21	0.01	0.03

Note. Analyses were carried out by V.A. Kreisberg and V.P. Rakcheev (Chemical Department of Moscow State University).
* Chemical etching of the sample was followed by its thermal crushing, which included heating of "superquartzite" to 900 ℃ and its subsequent rapid cooling in deionized water.
** "Superquartzite" after calcination at 1450 ℃ contains more high-temperature water than the Unimin standard samples.
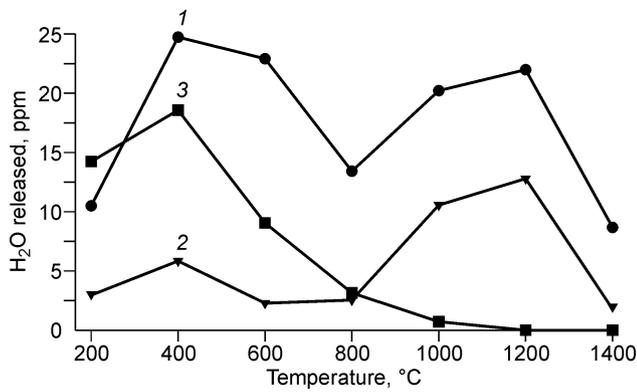
Fig. 2. Thermal desorption of water during the stepwise heating of "superquartzite" grit from the Bural-Sardyk deposit, with different thermal-treatment regimes (data of mass spectrometry analysis). *1*, sample 78/1, "superquartzite" without thermal crushing; *2*, sample 80/1, "superquartzite" after thermal crushing; *3*, sample 116/1, "superquartzite" after calcination at 1450 °C.
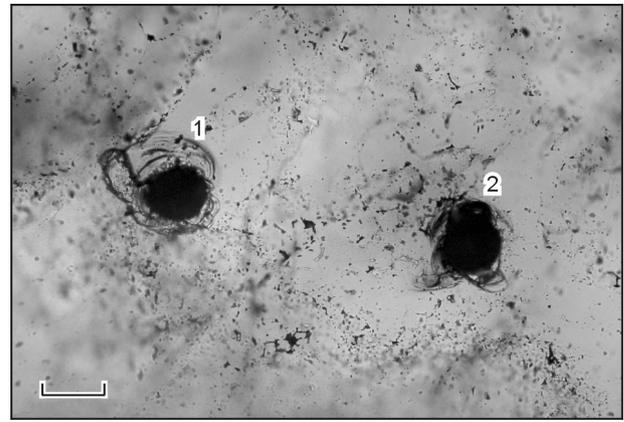

Fig. 3. Craters in the "superquartzite" zones analyzed by LA–ICP-MS. Crater 1, Optically pure zone; crater 2, zone with FI cluster. Measured with a 50 μm scale bar.

The contents of major elements in the "superquartzite" samples were calculated using the NIST SRM 612 synthetic glass (Jochum et al., 2011) as a standard. The measurements were made in series; each included laser ablation of the standard (an optically pure material) and the following analysis of an FI cluster. Each element content was calculated from the results of two parallel measurements.

Based on the recorded analytical signals, we evaluated the contents of major elements in the zones with FI clusters (Table 4). The contents of K, Li, B, and Ca in the optically pure zones and in the zones with FI clusters are nearly the same and vary only within the error of measurement. The content of Na in the zones with FI is an order of magnitude higher as compared with that in the pure zones (Table 4). That is, Na is the main alkaline element in the aqueous solution of FI. This is confirmed by the results of quartz concentrate enrichment (Table 5).

Table 5 presents the contents of impurities in the starting "superquartzite" and in the quartz concentrates obtained by

chemical enrichment of the quartz grit. The symbol Σ10 marks the total content of ten impurities specified for quartz concentrates. During the chemical enrichment following the thermal crushing of the sample, acid-soluble mineral inclusions are removed and the sample becomes free from Fe, Al, and K. The content of Na decreases insignificantly in the course of this process. After the calcination of the enriched quartz concentrate at 1450 °C, when the phase transformation of high-temperature quartz into cristobalite takes place (Zhaboedov et al., 2015) and FI are unsealed (the last line in Table 4), further chemical enrichment results in the drastic decrease in Na content. This confirms our conclusions (based on the LA–ICP-MS results) that Na is the main element in the salt system of the fluid.

Conclusions

The microcriothermometric, LA–ISP-MS, and ICP MS analyses have shown that the concentration of salts in the fluid

Table 4. Contents of major elements in "superquartzite" (from LA–ICP-MS data), ppm

Zone	^{7}Li	^{11}B	^{23}Na	^{24}Mg	^{27}Al	^{39}K	^{44}Ca
Optically pure	0.58	0.35	0.12	8.20	0.15	0.72	0.21
With FI clusters	0.67	0.39	1.04	6.02	0.24	0.61	0.24

Note. Analyses were carried out by N.V. Bryanskii and A.M. Makhlyanova at the Common-Use Center of Isotope-Geochemical Studies of the Institute of Geochemistry, Irkutsk.

Table 5. Contents of impurity elements in quartz concentrates, ppm

Analyte	Fe	Al	Ti	Ca	Mg	Cu	Mn	Na	K	Li	Σ10	P	B
Starting	6	27	1.7	0.8	1	0.17	0.02	3.5	6.3	0.13	46.6	0.2	0.2
After chemical enrichment	0.9	4.5	0.8	0.4	0.2	0.14	0.005	2.5	0.5	0.12	10.1	0.1	0.18
Calcination at 1450 °C + chemical enrichment	1.1	4	0.6	0.4	0.2	0.18	0.006	0.2	0.3	0.18	7.2	0.1	0.16

Note. Analyses were carried out by O.N. Solomein and V.Yu. Ponomareva at the Common-Use Center of Isotope-Geochemical Studies of the Institute of Geochemistry, Irkutsk.

corresponds to 5.5–5.7 wt.% NaCl equiv., Na is the main element in its salt system, and K and Mg are present in background concentrations.

The results of chemical enrichment of the "superquartzites" indicate low initial contents of structural impurities, which expands the boundaries for the application of this type of raw material in the production of high-tech quartz products.

The research was carried out at the Common-Use Center of Isotope-Geochemical Studies of the Institute of Geochemistry, Irkutsk.

References

Anfilogov, V.N., Kabanova, L.Ya., Igumentseva, M.A., Nikandrova, N.K., Lebedev, A.S., 2015. Geologic structure, petrography, and mineralogy of the Bural-Sa'rdag (East Sayan). Razvedka i Okhrana Nedr, No. 7, 18–23.

Arzhannikova, A.V., Jolivet, M., Arzhannikov, S.G., Vassalo, R., Chauvet, A., 2013. The time of the formation and destruction of the Meso–Cenozoic peneplanation surface in East Sayan. Russian Geology and Geophysics (Geologiya i Geofizika) 54 (7), 685–694 (894–905).

Bodnar, R.J., Vityk, M.O., 1994. Interpretation of microtermometric data for H_2O–NaCl fluid inclusions, in: De Vivo, B., Frezzotti, M.L. (Eds.), Fluid Inclusions in Minerals: Methods and Application. Virginia Tech, Pontignano–Siena, pp. 117–130.

Brown, P.E., 1989. FLINCOR: A microcomputer program for the reduction and investigation of fluid-inclusion data. Am. Mineral. 74, 1390–1393.

Bur'yan, Yu.I., Borisov, L.A., Krasil'nikov, P.A., 2007. Raw quartz, crucial mineral resources for high-tech industrial fields. Razvedka i Okhrana Nedr, No. 10, 9–12.

Fedorov, A.M., Makrygina, V.A., Budyak, A.E., 2012. New data on the geochemistry and mechanism of formation of quartzites of the Bural-Sar'dag deposit (Eastern Sayan Mountains). Dokl. Earth Sci. 442 (1), 120–125.

Jochum, K.P., Weis, U., Stoll, B., Kuzmin, D., Yang, Q., Raczek, I., Jacob, D.E., Stracke, A., Birbaum, K., Frick, D.A., Günther, D., Enweiler, J., 2011. Determination of reference values for NIST SRM 610-617 glasses following ISO Guidelines. Geostand. Geoanal. Res. 35 (4), 397–429.

Kreisberg, V.A., Rakcheev, V.P., Serykh, N.M., Borisov, L.A., 2007. Mass-spectrometric identification of gas–liquid impurities in quartz. Razvedka i Okhrana Nedr, No. 10, 12–18.

Kuznetsov, A.B., Letnikova, E.F., Vishnevskaya, I.A., Konstantinova, G.V., Kutyavin, E.P., Geletii, N.K., 2010. Sr chemostratigraphy of carbonate sedimentary cover of the Tuva–Mongolian microcontinent. Dokl. Earth Sci. 432 (1), 577–582.

Kuzmichev, A.B., 2004. Tectonic History of the Tuva–Mongolian Massif: Early Baikalian, Late Baikalian, and Early Caledonian Stages [in Russian]. PROBEL-2000, Moscow.

Kuzmichev, A.B., Larionov, A.N., 2011. The Sarkhoi Group in East Sayan: Neoproterozoic (~770–800 Ma) volcanic belt of the Andean type. Russian Geology and Geophysics (Geologiya i Geofizika) 52 (7), 685–700 (885–895).

Makhlyanova, A.M., Bryanskii, N.V., Nepomnyashchikh, A.I., 2015. Application of laser ablation to ICP MS study of gas–liquid inclusions in natural quartz. Izvestiya RAN. Seriya Fizicheskaya 79 (2), 203–206.

Makrygina, V.A., Fedorov, A.M., 2013. Quartzite transformation as a consequence of late tectonic events in the evolution of the Chuya and Gargan blocks. Russian Geology and Geophysics (Geologiya i Geofizika) 54 (12), 1450–1457 (1861–1870).

Sokol'nikova, Yu.V., Vasil'eva, I.E., 2012. Choice of the conditions of chemical sample preparation for ICP MS analysis of quartzites. Vestnik IGTU, No. 1, 119–127.

Vorob'ev, E.I., Spiridonov, A.M., Nepomnyashchikh, A.I., Kuz'min, M.I., 2003. Superpure quartzites of the Eastern Sayan (Buryat Republic, Russia). Dokl. Earth Sci. 390 (4), 497–500.

Zhaboedov, A.P., Nepomnyashchikh, A.I., Seredkin, E.A., 2015. Phase transitions in quartzites of the Bural-Sardyk deposit. Izvestiya Vuzov. Prikladnaya Khimiya i Biotekhnologiya, No. 4, 61–66.

Editorial responsibility: N.V. Sobolev